https://doi.org/10.32762/eygec.2025.1

# THE INFLUENCE OF THE TYPE OF CYCLIC SHEARING ON THE BEHAVIOUR

# João Pedro OLIVEIRA<sup>1</sup>, Luis ARAÚJO SANTOS<sup>2</sup>, Paulo COELHO<sup>3</sup>

#### **ABSTRACT**

Mining generates large volumes of waste, often stored in tailings dams, which pose risks under seismic loading. The undrained cyclic behaviour of these materials remains poorly understood, as triaxial tests fail to replicate real seismic conditions. This study compares the cyclic response of ore tailings using triaxial tests and the Hollow Cylinder Apparatus (HCA), which enables independent stress control and realistic loading paths. Reconstituted samples were used to ensure consistent initial conditions. Results highlight the influence of loading conditions on undrained behaviour, emphasising the importance of realistic testing for tailings dam stability in seismic regions.

Keywords: mine tailings, triaxial test, hollow cylinder apparatus, cyclic loading.

#### INTRODUCTION

The transition to a sustainable society increases the demand for minerals and metals, potentially doubling or quadrupling mineral consumption by 2040 (De Jong, 2021). The mining industry already generates large volumes of tailings, which will certainly continue to grow. These are typically stored in dams, where seismic liquefaction is a major cause of failure. Liquefaction can occur due to reduced shear strength after an earthquake, even without extreme seismic loads. Tailings dams, subjected to multiple earthquakes over time, may experience behavioural changes, as seen in the Kayakari dam in Japan, which liquefied in 2011 despite withstanding the 2003 earthquake (Ishihara et al., 2011). This study assesses the cyclic response of tungsten tailings using triaxial tests and the Hollow Cylinder Apparatus (HCA) to compare undrained cyclic behaviour under pure horizontal shear.

# STATIC AND CYCLIC LIQUEFACTION

Liquefaction is a complex and debated topic in Geotechnical Engineering (Kramer, 1996), occurring pressures large excess-pore-water reduce the effective stresses in the soil. Two key phenomena are flow liquefaction and cyclic mobility. Flow liquefaction, though rarer but more destructive (Kramer, 1996), transforms soil into a liquid state due to excess pore pressure, as seen in the Brumadinho dam failure (Robertson et al., 2019). Cyclic mobility occurs when static shear stress is lower than the liquefied soil's shear strength (Kramer, 1996) and can be triggered by cyclic loading, leading to large ground oscillations during seismic events.

Araújo Santos (2015) conducted cyclic torsion tests on Coimbra sand, a granular material, using the HCA, as shown in Figure 1.

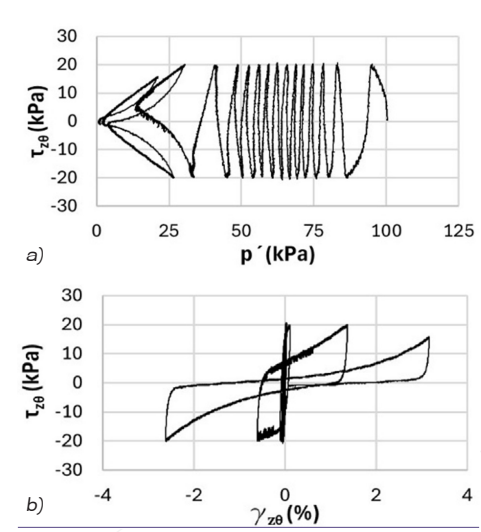


Figure 1 Torsional test with Coimbra sand (Adapted from Araújo Santos, 2015): a) stress paths; b) Stress-strain curves

As illustrated in Figure 1a, liquefaction by cyclic mobility was observed, evidenced by the progressive reduction of effective stresses (p') with the increasing number of cycles. When subjected to cyclic torsional loading  $(\tau_{z_0})$ , the sand exhibited hysteretic loops characteristic of this type of loading (Figure 1b).

<sup>1</sup> PhD Student, University of Coimbra, Coimbra, Portugal, joaopsvo@uc.pt

<sup>2</sup> PhD, Adjunct Professor, Polytechnic University of Coimbra, SUScita, Coimbra, Portugal, Imsantos@isec.pt

<sup>3</sup> PhD, Assistant Professor, University of Coimbra, CITA, Coimbra, Portugal, pac@dec.uc.pt

#### MATERIAL UNDER STUDY

The material used in this work was collected from a Portuguese mine and served solely as an example of mining tailings, with no incidents occurring in its storage structures. The tailings come from the Panasqueira mine, which primarily exploits tungsten, tin, and some copper. The collected tailings are representative of the material deposited in one of the mine's tailings dams.

The initial characterisation of the material included determining the density of solid particles, particle size distribution, and Atterberg limits. The density of solid particles (G) was determined as 3.15, the liquid limit ( $w_{\rm L}$ ) as 23.3%, and the plastic limit ( $w_{\rm p}$ ) as 14.7%, in accordance with the applicable national and European standards. The obtained parameters fall within the typical range for these geomaterials, with some variations in particle size distribution due to the milling process and the type of ore extracted. Figure 2 illustrates the particle size distribution of the tailings under study.

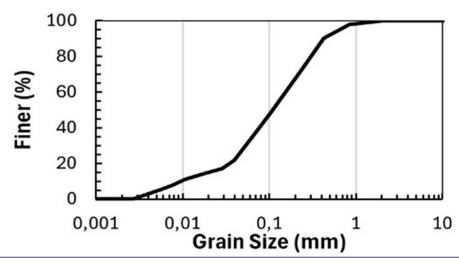


Figure 2 Grain size of Panasqueira mine tailings

The average particle size curve shows  $D_{_{60}}\approx 0,149$  mm, and  $D_{_{10}}\approx 0.014$ mm, with a uniformity coefficient (C $_{_{0}}$ ) of 10,64 and a curvature coefficient (C $_{_{0}}$ ) of 1.78. According to the average particle size curve, the tailings consist of 70% sand and 30% silt and can be classified as silty sand (SM).

#### PREPARATION OF RECONSTITUTED SAMPLES

Based on the technique proposed by Carraro and Prezzi et al. (2008), an apparatus was developed to mechanically mix the tailings with water and obtain a truly homogeneous slurry mixture. The operation consists of introducing the mining tailings and water into a metal mixing tank and operating it for 2 minutes, using a specially designed blade to achieve a deep and uniform mix. A water content of 27% was chosen to ensure a continuous and homogeneous deposition of the paste. After the selected period, the mixer is switched off, and the tap located at the bottom of the metal tank is opened to allow the paste to flow by gravity into the mould of the sample to be tested. This equipment facilitates the reconstitution of uniform samples of different sizes and shapes, including solid cylindrical samples for the triaxial test and hollow cylindrical samples for the HCA.

#### LABORATORY EQUIPMENT

The cyclic triaxial tests on the 38D:76H samples (D - diameter; H - height in mm) were conducted in a stress path cell, shown in Figure 3a, capable of reaching maximum stresses of 1000 kPa. The sample, insulated by a membrane, rests on a pedestal connected to the piston, with suction applied to the load cell via a rubberized connecting cap. The pedestal moves vertically in both directions, controlled by a constant rate of strain pump (CRSP) generating constant strain rates. The 60ID:1000D:200H (ID - internal diameter, OD - outer diameter, H - height in mm) hollow samples were tested using the HCA at the University of Coimbra (UC), shown in Figure 3b. The University of Coimbra uses the HCA Mark II (Ramos et al., 2019), which allows for control of the principal stress direction and measures deformation at both small and large





Figure 3 Equipment used: a) Stress Path Cell; b) Hollow Cylinder Apparatus at UC

## **RESULTS**

The stress-strain response and shear strength of the samples reconstituted using the slurry deposition method were evaluated by comparing an undrained cyclic triaxial compression test with an undrained cyclic torsional test. To ensure comparability between both tests, the axial stress difference (q) and axial strain  $(\epsilon_{_{\alpha\nu}})$  from the triaxial tests were converted into maximum shear stress  $(\tau_{\text{\tiny max}})$  and shear strain (γ), respectively. This transformation accounts for the differences in the orientation of the principal stresses in each test: in the triaxial test, the principal stresses vary between 0° and 90°, while in the test conducted with the HCA, the direction of the principal stresses remains constant at 45°, allowing for the analysis of the effects of stress plane rotation. The conversion follows established relationships, where the shear stress in triaxial conditions is given by  $\tau_{\text{max}}=q/2$  and the shear strain is approximated as  $\gamma \cong$ 3/22... Both samples were isotropically consolidated under a confining stress of 100 kPa before testing.

The sample tested in the triaxial apparatus was subjected to cyclic loading of  $\Delta \tau$ =±20 kPa. The stress trajectory (Figure 4a) shows that the first loading

cycle generates larger excess pore pressure, significantly reducing the effective stress.

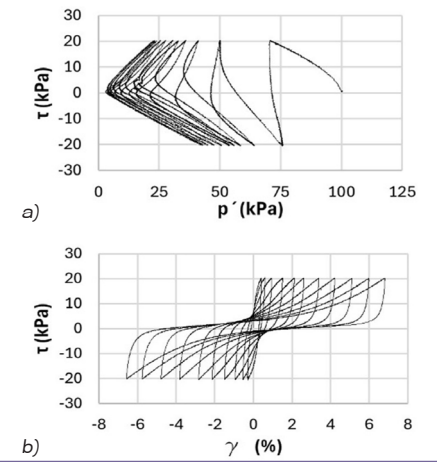


Figure 4 Cyclic Triaxial test: a) stress paths; b) Stress-strain curves.

The sample exhibits progressive decrease in effective stress due to continuous excess-pore-pressure generation. As the cycles progress, the mean effective stress approaches zero, forming a "butterfly" shape typical of cyclic liquefaction. The axial stress-strain response (Figure 4b) initially indicates high stiffness, but with increasing cycles, shear stiffness degradation and strain accumulation become evident. Unlike the observations of Coelho et al. (2024), the deformations in this study remain fairly symmetrical, with no greater strain accumulation in extension.

The torsional test conducted in the HCA (Figure 5) was carried out under constant radial and mean principal stress. A cyclic torsional shear stress of  $\Delta\tau_{\rm y}$ -  $\pm$  20 kPa was applied (Figure 5a).

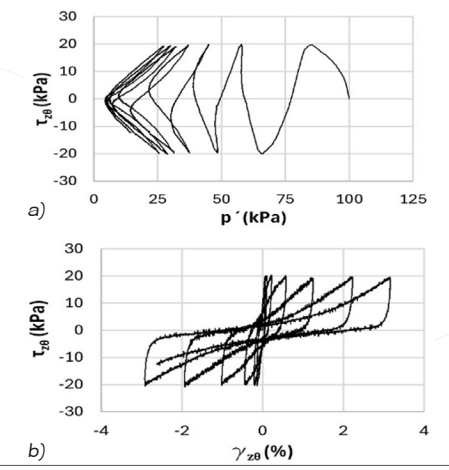


Figure 5 Torsional test: a) stress paths; b) Stressstrain curves

Here, the stress and strain variables are expressed as  $\tau_{z_0}$  and  $\gamma_{z_0}$ , reflecting the different shear plane orientation in torsional loading.

The response was nearly symmetrical in both deformation and stress path. Figure 5a shows that the first cycle generated higher excess pore pressure, reducing the effective stress, similar to the cyclic triaxial test (Figure 4) and consistent with findings in other granular materials. The stress-strain curve (Figure 5b) suggests progressive energy dissipation and stiffness loss, likely due to particle reorganisation throughout the cycles. Initially, the geomaterial exhibited a hardening behaviour, with relatively high stiffness during the early deformations. As the deformations increased, a transition to a softening regime was observed, characterised by the progressive degradation of stiffness and an increase in accumulated deformation. According to Araújo Santos (2015), the stress path significantly influences the mechanical response, with induced anisotropy and principal stress rotation being key factors in the evolution of strength and stiffness.

Figure 6 illustrates the variation of the mean effective stress during the tests by plotting the values of effective confining stress, normalised by its initial value (p'/p'<sub>n</sub>), at the beginning of each cycle against the shear strain, for the two tests performed. Only the first seven cycles were analysed, as they correspond to a double amplitude strain of 5% and marked the end of the HCA test. The figure shows that both tests follow a nonlinear decreasing trend that reflects the effective stress loss in each cycle. Up to the third cycle, they exhibit similar behaviour; however, from that point onwards, the test conducted in the HCA shows a more rapid degradation up to the seventh cycle. This difference can be attributed to the direction of the principal stresses, as explained earlier, with the triaxial test applying the principal stresses differently compared to the HCA. According to some studies, the HCA provides a more realistic representation of field conditions and is particularly advantageous in assessing liquefaction in sandy soils.

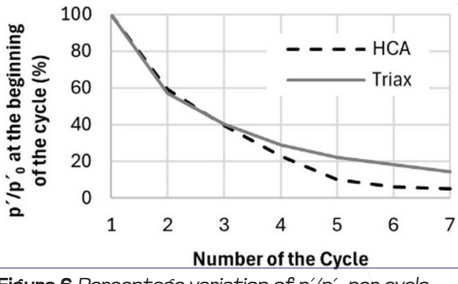


Figure 6 Percentage variation of p'/p', per cycle

The lines represented in Figure 7 illustrate the evolution of maximum and minimum strains with the number of cycles in both tests performed.

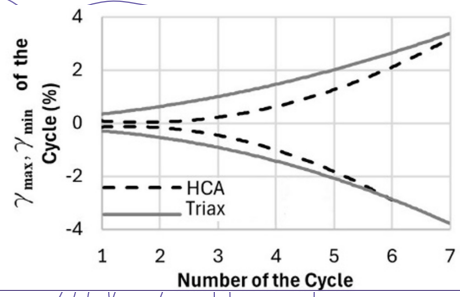


Figure 7 Percentage  $\gamma_{\text{max}}$ ,  $\gamma_{\text{min}}$  per cycle

The curves show that, in the triaxial test, the strains increase more rapidly, and their double amplitude is slightly higher, indicating a faster softening of the soil. In the HCA, the strains are initially smaller but difference decreases as cycles progress. On the other hand, in both tests, the maximum and minimum strains exhibit symmetry. These results differ from other studies on reconstituted soils, where cyclic triaxial tests typically show greater accumulation of strain in extension than in compression (Coelho et al., 2024). In contrast, due to the influence of progressive stress rotations as opposed to the sudden inversion of stress directions that takes place in the triaxial test, the stress-strain response observed in the HCA tends to exhibit greater strain symmetry (Araújo Santos, 2015).

# CONCLUSIONS

The cyclic tests conducted on tungsten tailings using triaxial equipment and the HCA revealed some similarities in behaviour, considering the different stress paths and failure planes. The triaxial test exhibited a faster softening and slightly higher strains per cycle, whereas the HCA showed lower strain magnitudes. In both tests, a symmetry between positive and negative strains was evident, highlighting that, in the triaxial test, this result contrasts with other published studies on different types of tailings. This difference may be attributed to the mineralogy and grain size distribution of tungsten tailings, which influence the material's mechanical response, as well as the sample reconstitution method, which may have resulted in a more stable initial structure. Furthermore, the independent stress control in the HCA allows for more realistic stress paths, including principal stress rotation, which may have contributed to the greater strain symmetry observed in this test. These findings emphasise the importance of selecting an appropriate testing method when assessing the cyclic response and liquefaction potential of sandy soils, reinforcing the relevance of the HCA in simulating more fieldrepresentative conditions.

#### **ACKNOWLEDGMENTS**

The authors acknowledge the financial support of the FCT for the GeoSusTailings Project (PTDC/ECI-EGC/4147/2021) and the collaboration of Beralt Tin and Wolfram Portugal, S.A., for supplying the tungsten tailings for testing.

### REFERENCES

- Araújo Santos, L. (2015). Characterization of the mechanical behaviour of Coimbra sand under generalized loading. PhD thesis, Coimbra Univ., Portugal (in Portuguese).
- Carraro, J., Prezzi, M., (2008). A New Slurny-Based Method of Preparation of Specimens of Sand Containing Fines, Geotechnical Testing Journal, 31, n°1:111.
- Coelho, P., Camacho, D. (2024). The Experimental Characterization of Iron Ore Tailings From a Geotechnical Perspective. Appl. Sci. 2024, 14.
- De Jong, T., Sauerwein, T., Wouters L. (2021). Mining and the Mining and the Green Energy Transition: Review of International Development Challenges and Opportunities.» Washington, US, USAID.
- Ishihara, K., Ueno, K., Yamada, S., Yasuda, S., Yoneoka, T. (2011). Breach of a tailings dam in the 2011 earthquake in Japan. Soil Dynamics and Earthquake Engineering, 31, 2.
- Kramer, S. (1996). Geotechnical Earthquake Engineering. 1st Edition, Prentice Hall, Upper Saddle River, New Jersey.
- Ramos, R. C., Coelho, P., Araújo Santos, L. (2019). The use of the Hollow Cylinder Apparatus in the study of liqueflable soils. Earth. Geotechnical Eng. for Protection and Development of Environment and Constructions, Rome, Italy.
- Robertson, P. K., Melo, L., Williams, D. J., Wilson, G. W. (2019). Report of the Expert Panel on the Technical Causes of the Failure of Feijão Dam I.